Macromolecules
Cite This: Macromolecules 2019, 52, 8662−8671
Article
pubs.acs.org/Macromolecules

Topology Analysis of Chain Walking Polymerized Polyethylene: An Alternative Approach for the Branching Characterization by Thermal FFF

Martin Geisler,[†,‡] William C. Smith,[§] Laura Plüschke,[†,‡] Robert Mundil,[∥] Jan Merna,[∥] S. Kim Ratanathanawongs Williams,[§] and Albena Lederer*[,†,‡]

[†]Polymer Separation Group, Leibniz-Institut für Polymerforschung Dresden e. V., Hohe Str. 6, 01069 Dresden, Germany
[‡]Faculty of Chemistry and Food Chemistry, Technische Universität Dresden, 01062 Dresden, Germany
[§]Department of Chemistry, Colorado School of Mines, Golden, Colorado 80401, United States
[∥]Department of Polymers, University of Chemistry and Technology Prague, Technická 5, 166 28 Praha 6, Czech Republic

Supporting Information

ABSTRACT: Thermal field-flow fractionation (ThFFF) was designed to investigate the retention behavior of a series of dendritic polyethylenes synthesized using a chain walking catalyst (cwPE) with variations in the branching architecture. The retention behavior of these macromolecules correlates with their branching. Based on differences in the Soret coefficient, a new model has been developed for the application of ThFFF as an alternative to the branching calculation approach based on light scattering or viscosity for the branching analysis of novel short-chain branched PEs.

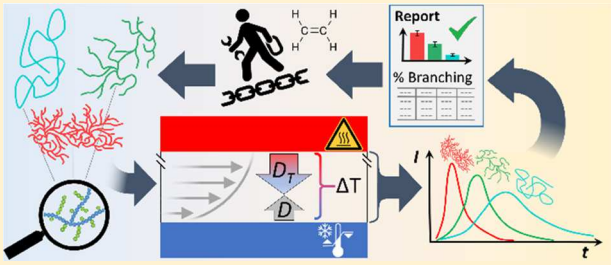

INTRODUCTION

Polyethylene (PE) represents a multibillion dollar industry[1,2] each year as a polymer widely used in multiple applications. Fine-tuning of the molar mass and molecular topology enables control over processing and mechanical properties. These optimized materials are nowadays readily accessible due to the progress in catalyst development since Ziegler−Natta in the 1950s.[3] However, an in-depth understanding of the molecular size and topology in relation to the bulk properties of the polymers still needs to be developed. The often semicrystalline structure of polyolefins requires an analysis at elevated temperatures to enable sufficient solubility.[4] This solution behavior is the reason for time-consuming analytical approaches for the characterization of molecular topology, for example, fractionation according to the crystallization of PE such as temperature rising elution fractionation[5] and crystallization analysis fractionation.[6] Currently, the established characterization method of polyolefins is high-temperature size exclusion chromatography (HT-SEC), most commonly performed in chlorinated aromatic solvents such as 1,2,4-trichlorobenzene (TCB)[7,8] or in its recently introduced green substitute butylal.[9] Coupled to absolute molar mass detection methods, like multiangle light scattering (MALS), online viscometry, and dynamic light scattering (DLS) with concentration detectors,[10] a comprehensive characterization of the molar mass and branching is possible. The branching analysis introduced by Zimm and Stockmayer[11] proposes the definition of a contraction factor g, as shown in eq 1[11]

$$g = \left(\frac{R_{G,BRA}^{\ 2}}{R_{G,LIN}^{\ 2}}\right)_M = \left[\left(\frac{[\eta]}{[\eta]_{LIN}}\right)_M\right]^{1/\varepsilon} \quad (1)$$

where R_G is the radius of gyration or mathematically the root-mean-square radius (RMS) of the branched polymer and $R_{G,LIN}$ is the RMS radius of a linear polymer chain of the same molar mass and chemical structure. An alternative definition for a contraction factor g' defined as the quotient of the intrinsic viscosities of the sample $[\eta]$ and the linear analogue $[\eta]_{LIN}$ has been introduced later,[12] in that the drainage exponent ε has been found to be dependent on the branching type.[13−15] g can be expressed as a function of the number of branches per molecule (B). For a randomly branched monodisperse trifunctional polymer, g (index 3 for trifunctional) is described as given in eq 2[11]

$$g_3 = \left[\left(1 + \frac{B}{7}\right)^{0.5} + \frac{4B}{9\pi}\right]^{-0.5} \quad (2)$$

Several parameters have been defined to enable an easy comparison between macromolecules of the same chemical origin, but different topologies. One parameter is the number of long-chain branches per 1000 monomers (LCB) as defined in eq 3

Received: July 8, 2019
Revised: September 19, 2019
Published: November 5, 2019

DOI: 10.1021/acs.macromol.9b01410
Macromolecules 2019, 52, 8662−8671

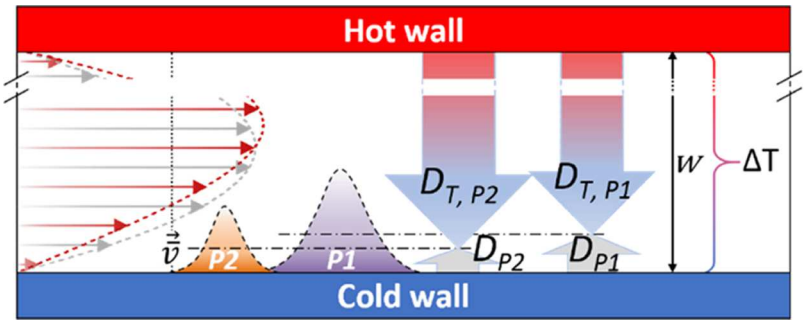

Figure 1. Schematic separation of two analytes *P*1 and *P*2 in the laminar flow of a thin ThFFF channel with thickness *w*, separated by a difference in their counteracting mass transports described by D_T and *D* in the separation force field ΔT. The flow profile in gray shows a laminar profile without field; the distorted flow profile with the applied field is shown in red.

$$\mathrm{LCB} = 1000 \times B \times \frac{M_{\mathrm{RU}}}{M} \tag{3}$$

where *M* is the molecule molar mass and M_{RU} is the molar mass of a repeat unit. In this work, a value of M_{RU} = 28.05 g mol^{-1} has been chosen for polyethylene referring to one ethylene monomer as the repeat unit within the polymer chain.

Additionally, the theoretical molar mass of a long-chain branch segment eq 4 can be used as an alternative branching expression of a polymer molecule

$$M_{\mathrm{Seg}} = \frac{M}{(B+2)+(B-1)} = \frac{M}{2B+1} \tag{4}$$

where the term $(B + 2)$ represents segments at a terminal position and $(B - 1)$ segments in between two branching points.[16,17] The number of branches *B* for the calculation of M_{Seg} in eq 4 is accessible by the transformation of eq 2.

The introduction of late transition metal catalysts opened a novel route for the synthesis of short-chain branched polyolefins via the chain walking mechanism with precisely defined macroscopic topologies.[18,19] These polyolefins have special local structural characteristics containing a constant amount of branches of about 50−60 per 1000 monomers. This specific structure defines the bulk and solution properties of these polymers.[20] However, the structure−property relationship of this entirely different polyethylene is not yet comprehensively understood. Nevertheless, it opens an opportunity to investigate alternative ways for the branching analysis due to their very low crystallinity or even amorphous structure and their good solubility in a variety of rather untypical PE solvents, such as cyclohexane (CHX), chloroform, and tetrahydrofuran (THF), even at low temperatures.[10,18,21,22] Furthermore, the absence of functionalities at the branch ends and the variation of branching[23,24] makes a straightforward investigation possible, based only on the branching architecture.

THERMAL FIELD-FLOW FRACTIONATION (THFFF)

In SEC, the separation is based on entropically driven diffusivity of the analytes and depends on their hydrodynamic volume.[25] However, SEC may become challenging if the samples are far beyond the separation range and if interactions with the column packing material or, typically for highly branched structures, anchoring effects may occur, which lead to a co-elution of linear and less-branched fractions with highly branched fractions of different hydrodynamic sizes.[26] Unlike SEC, field-flow fractionation (FFF) provides a variety of advantages for the separation of branched and hyperbranched structures due to the absence of a column packing material.[27] Depending on the FFF method, different separation mechanisms have been explored.[28] In all FFF techniques, the principle of the separation is based on a laminar flow through a thin ribbon-like channel. Perpendicular to the flow direction, a separation force field is applied, causing retention of an analyte due to its response to the field. This response induces mass transport, which is counterbalanced by the translational diffusion caused by the Brownian motion.[28]

In ThFFF, the separation force is provided by a temperature gradient between a heated and actively cooled wall of the channel. The basic separation principle is illustrated in Figure 1. The process describing the response of molecules or particles to a temperature gradient is called thermophoresis and has been described by Ludwig and Soret in the late 19th century.[29,30] A variety of different theoretical approaches have been developed to describe this phenomenon. However, thermal diffusion in liquids is sensitive to many different contributions, making an in-depth understanding still challenging.[31] For polymers in solution, the dependence of the thermophoretic mobility on the length of the Kuhn segment has been indicated recently.[32,33]

To express the strength of the response to the temperature field, the Soret coefficient S_T is defined as the ratio of the thermal diffusion coefficient D_T causing the accumulation of objects in solution/dispersion on either the hot (thermophilic) or the cold site (thermophobic) to the translational diffusion coefficient *D* caused by the Brownian motion. The dimensionless retention parameter λ in the FFF theory describes the ratio between the distance of the center of gravity of the analyte concentration distribution from the accumulation wall (mean layer thickness) and the channel thickness *w* for ThFFF and is defined in eq 6 by S_T and ΔT.

$$\lambda = \frac{1}{S_T \Delta T} = \frac{D_T}{D\,\Delta T} \tag{6}$$

With the parameters containing the field strength and the description of the analyte mass transport, the retention in ThFFF is then defined as given in eq 7

$$R = \frac{t_0}{t_R} = 6\lambda\left[\nu + (1 - 6\lambda\nu)\left(\coth\left(\frac{1}{2\lambda}\right) - 2\lambda\right)\right] \tag{7}$$

with *R* being the retention ratio, t_0 the void time describing the average flow time of the solvent or an unretained analyte, and t_R the retention time of a retained analyte. For careful work and in particular for less retained analytes, the general retention equation for ThFFF is modified by introducing a non-

DOI: 10.1021/acs.macromol.9b01410
Macromolecules 2019, 52, 8662−8671

Table 1. Summary of the Mean Results Obtained by HT-SEC−D4 and ThFFF (ΔT = 100.9 ± 0.7 K, τ = 10 min)[a]

	HT-SEC−D4					ThFFF				
	M_w/kg mol^{-1}	$Đ$	g_z	LCB$_w$	M_{Seg}/kg mol^{-1}	M_w /kg mol^{-1}	$Đ$	t_R/min	$S_T/10^1$ K^{-1}	$D_T/10^8$ cm^2 s^{-1} K^{-1}
hb1	230 ± 6	1.32	0.22 ± 0.01	18.8 ± 2.2	0.85 ± 0.04	205 ± 10	1.07	14.1 ± 0.7	0.32 ± 0.06	0.9 ± 0.2
hb2	161 ± 3	1.12	0.27 ± 0.01	14.3 ± 1.4	0.91 ± 0.05	166 ± 9	1.06	14.9 ± 0.9	0.37 ± 0.07	1.1 ± 0.2
b1	140 ± 3	1.02	0.55 ± 0.03	2.7 ± 0.3	4.35 ± 0.02	136 ± 7	1.06	30.2 ± 0.4	0.96 ± 0.08	2.2 ± 0.2
b2	136 ± 2	1.03	0.55 ± 0.01	3.2 ± 0.4	2.97 ± 0.21	131 ± 5	1.03	24.5 ± 0.1	0.77 ± 0.07	1.9 ± 0.2
sb	313 ± 9	1.08	0.49 ± 0.02	1.5 ± 0.1	8.61 ± 0.40	307 ± 16	1.08	39.2 ± 1.0	1.33 ± 0.11	2.1 ± 0.2
lin1	175 ± 1	1.06	0.53 ± 0.01	2.2 ± 0.1	6.36 ± 0.20	167 ± 11	1.04	36.8 ± 0.4	1.14 ± 0.11	2.3 ± 0.3
lin2	384 ± 7	1.11	0.54 ± 0.01	1.1 ± 0.4	17.5 ± 2.0	373 ± 14	1.07	56.6 ± 0.4	1.8 ± 0.2	2.5 ± 0.3

[a]All averages are calculated from n = 3; uncertainties represent overall deviation-inclusive systematic errors (see SI).

parabolicity factor ν describing the deformation of the flow profile depending on the field strength due to the changing viscosity of the carrier fluid eq 7.[34,35]

In contrast to the flow field-flow fractionation (FlFFF),[36−38] the separation of ThFFF is driven by thermophoresis and is mainly dependent on the chemical composition of analytes.[39] This dependence was already shown by Schimpf and Giddings using ThFFF[40] and by Köhler and Rauch by thermal diffusion-forced Rayleigh scattering (TDFRS) for polymers.[41] These properties depend only weakly on the size or molar mass and become even independent of them above a certain size.[41] Although thermal diffusion was assumed to be independent of the molar mass and branching,[42] in later reports, it was demonstrated that ThFFF can be used for the separation and analysis of differently branched polymers even if they are of the same size or molar mass.[43−46] However, due to the need of elevated temperatures, for polyolefins, only a few investigations with ThFFF have been performed in the past showing the potential of this method,[47,48] but without focusing on the influence of branching on the thermal diffusion behavior.

EXPERIMENTAL SECTION

Detailed information about the synthesis, the ThFFF instrumentation, and experimental conditions for ThFFF separations is given in the Supporting Information (SI).

RESULTS AND DISCUSSION

Characterization by HT-SEC−D4. Prior to the ThFFF experiments, the short-chain branched cwPE samples have been comprehensively analyzed by high-temperature size exclusion chromatography coupled to a fourfold detection system (HT-SEC−D4)[10] to obtain reliable molecular parameters and to validate the expected topology according to the conditions used for their synthesis. The results obtained by HT-SEC−D4 are summarized in Table 1. Molar mass calculations were carried out using a refractive index increment for PE in TCB at 150 °C of $dndc^{-1}$ = −0.104 mL g^{-1} taken from the literature.[49,50] Due to the unavailability of an entirely soluble, absolutely linear sample without short-chain branches or an absolutely well-defined sample without any long-chain branches and to retain the comparability to previous works, well-established theoretical models with $R_{G,LIN}$ = 0.023 $M^{0.58}$ and $[\eta]_{G,LIN}$ = 0.053 $M^{0.70}$ have been used for the branching calculations.[10,51,52] The samples have been named according to their expected topology with hb for hyperbranched, b for branched, sb for slightly branched, and lin for rather linear structures.

The influence of the synthesis conditions on the molecular topology was confirmed by HT-SEC−D4 in this investigation. Thus, a low pressure leads to highly branched samples while a

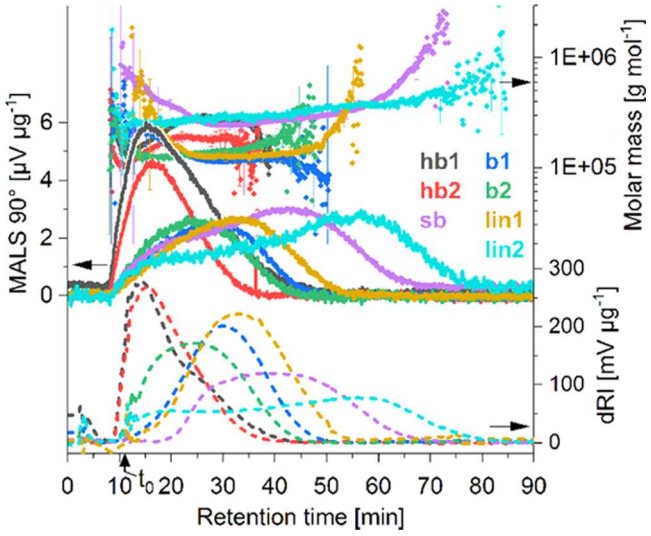

Figure 2. Superimposed fractograms of seven cwPEs with different topologies ranging from linear to dendritic, separated in a field of ΔT = 100.9 ± 0.7 K with a stop-flow of τ = 10 min. The temperature of the cold wall was kept at T_c = 23.0 ± 0.04 °C.

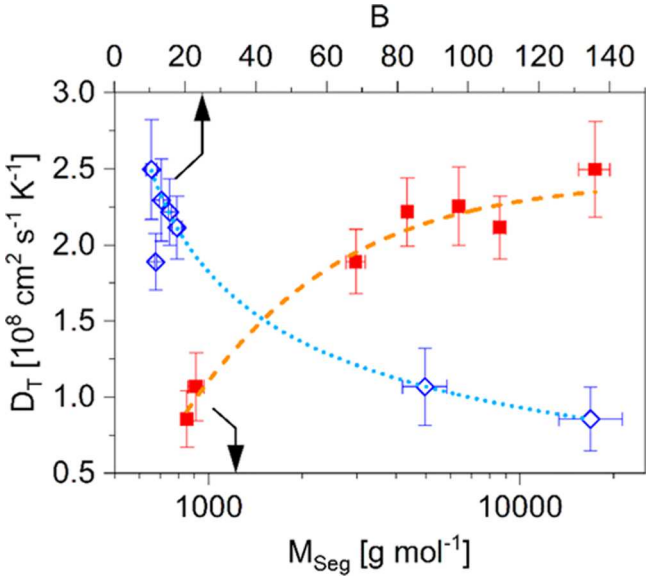

Figure 3. Dependence of D_T on the polymer topology: D_T vs B and vs M_{Seg}. B and M_{Seg} were calculated from HT-SEC−D4 data and temperature-dependent DLS data (measured in batch). The dotted and dashed red lines are for guiding the eye. The shown D_T are measured at ΔT = 100.9 K and τ = 10 min.

DOI: 10.1021/acs.macromol.9b01410
Macromolecules 2019, 52, 8662−8671

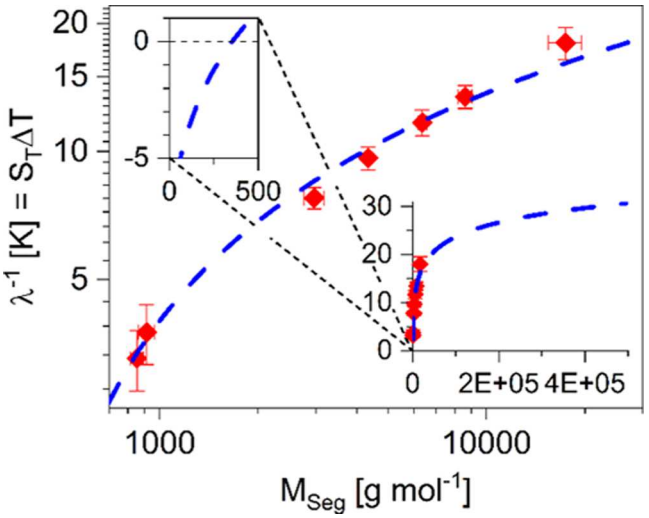

Figure 4. Double logarithmic plot of λ^{-1} against M_{Seg} from the data measured at ΔT = 100.9 K and τ = 10 min, fitted with a natural logarithmic function $y = a \ln(x) + b$. The inset shows the continuation of the fits to M_w, and the enlarged view of the inset indicates the trend toward negative S_T values for M_{Seg}, as shown previously for *n*-alkanes.[32]

Table 2. Branching Analysis Results Obtained by eqs 8−10 from ThFFF at ΔT = 100.9 ± 0.7 K and τ = 10 min and HT-SEC−D4 Weight Average g_w for Comparison with the g'' Estimated from ThFFF dRI Peak Apexes[a]

	ThFFF			HT-SEC−D4
	g''	$g = f(g'')$	LCB = $[g(g'')]$	g_w
hb1	0.11 ± 0.02	0.21 ± 0.03	18 ± 4	0.21 ± 0.01
hb2	0.13 ± 0.02	0.25 ± 0.04	17 ± 4	0.25 ± 0.01
b1	0.39 ± 0.03	0.50 ± 0.01	3.6 ± 0.5	0.50 ± 0.01
b2	0.30 ± 0.03	0.45 ± 0.01	4.4 ± 0.3	0.46 ± 0.02
sb	0.44 ± 0.04	0.52 ± 0.02	1.4 ± 0.2	0.48 ± 0.02
lin1	0.46 ± 0.04	0.54 ± 0.01	2.6 ± 0.3	0.53 ± 0.01
lin2	0.62 ± 0.07	0.57 ± 0.01	0.9 ± 0.1	0.57 ± 0.03

[a]See footnote of Table 1.

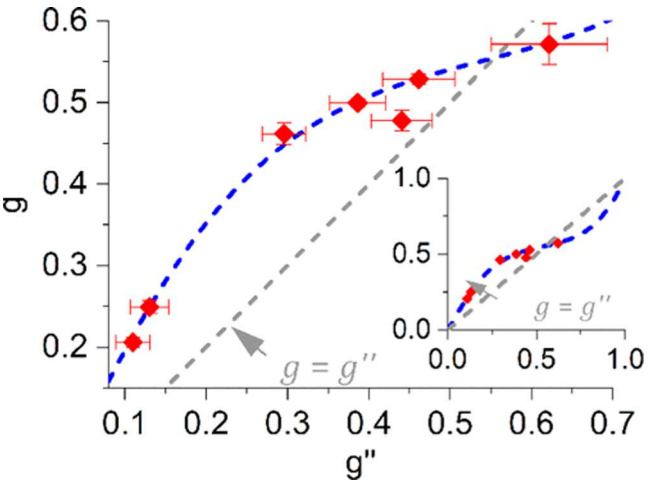

Figure 5. Comparison of g and g'' (data given in Table 2) and the fit to transform g'' into g for further calculations, shown for ΔT = 100.9 K and τ = 10 min. The inset shows the plot in the full scale within the limits of 0 and 1 for the fit in eq 10.

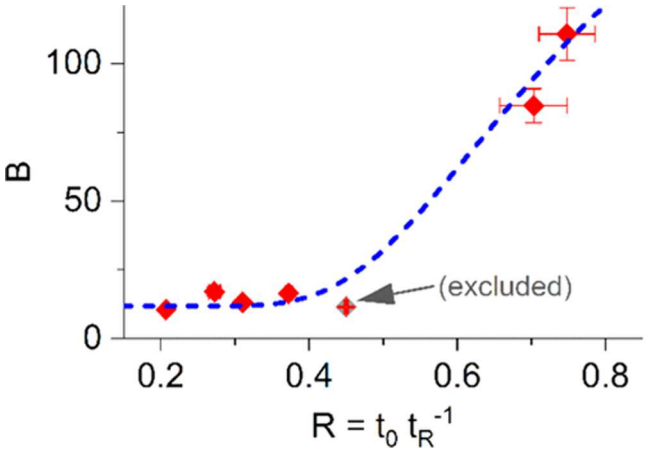

Figure 6. Dependence of $t_{R,\ dRI\ apex}$ on the number of branches per molecule B for ΔT = 100.9 K and τ = 10 min. The dashed lines indicate the fit by eq 13. The comparison of the data and fit parameters between the relaxed/unrelaxed systems and different field strengths is given in Figure S10, SI.

high pressure leads to almost entirely linear structures. Instead, higher reaction temperatures lead to generally higher molar masses than lower ones, but their influence on the resulting topology is not significant.[10,22,53] The chromatograms and detailed results of the branching analysis can be found in the SI.

Characterization by ThFFF. In our previous investigations, we successfully used THF as the carrier fluid in SEC under ambient conditions to characterize the molecular properties of the cwPE,[10,22] which needs much lesser technical effort than HT-SEC−D4. Therefore, our first attempt was to use THF as an eluent in ThFFF; however, under these conditions, no significant retention was observed even at increasing ΔT. Assumptions by the Hansen solubility theory using the solubility parameters of commercial PE indicated CHX as a thermodynamically good, nonhygroscopic solvent.[54] Retention experiments at two different isocratic ΔT values confirmed the suitability of CHX as a carrier liquid enabling reasonable retention for all PE samples, as shown in Figure 2. A significant difference in retention was observed depending on the molecular topology found by HT-SEC−D4. Furthermore, a dependence of the relaxation time on the length of the linear chain has been found indirectly (Figure S6, SI). For the presented differential refractive index (dRI) signals as the concentration source, a subtraction of separately recorded blank-baselines has been applied.

The narrow molar mass dispersity[55,56] $Đ = M_w M_n^{-1}$ of the samples allows for the investigation of the relation between the polymer topology and thermal diffusivity as a model system. Generally and in this work, the index n refers to the number-average, w to the weight-average, and z to the z-average moments of the regarded quantity.[55,57] The Soret coefficients S_T in Table 1 were calculated based on the mean retention times t_R's of the MALS and dRI peak apexes merged using a numerically derived polynomial solution given in the SI with respect to the distortion of the flow profile even for poorly retained analytes. The ΔT value used in the calculations is the cumulative average of the recorded $\Delta T(t_{R,i})$ from t_0 to the considered t_R. The given thermal diffusion coefficients D_T were calculated from S_T with translational diffusion coefficients D, which were determined at the corresponding mean layer

DOI: 10.1021/acs.macromol.9b01410
Macromolecules 2019, 52, 8662−8671

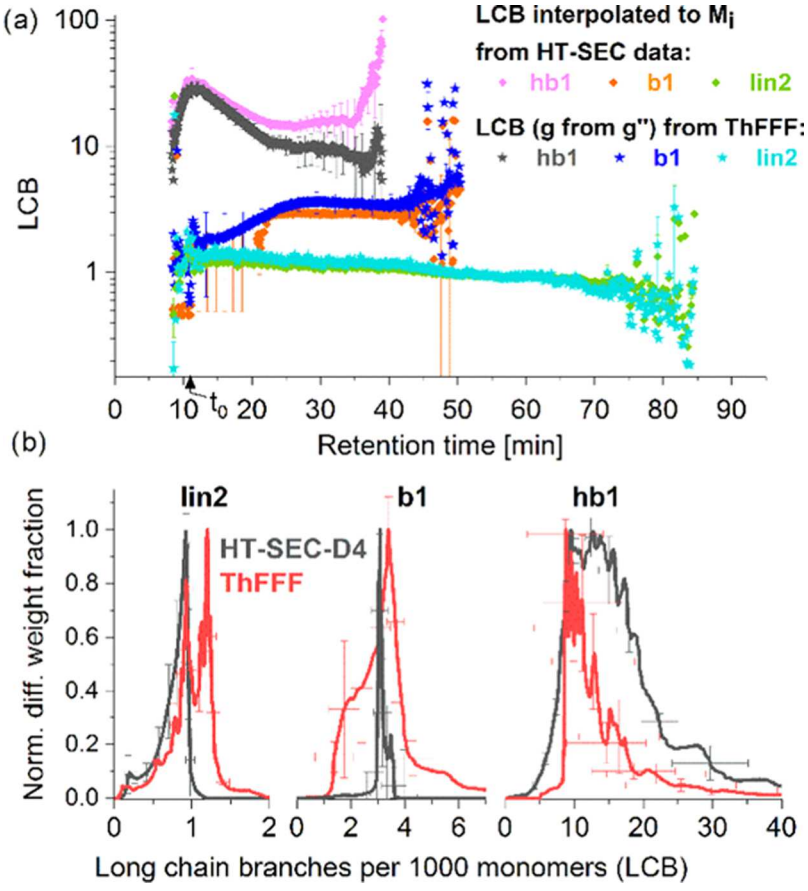

Figure 7. (a) Superimposed LCB_i from the ThFFF data (shown for ΔT = 100.9 K and τ = 10 min) and LCB_i from HT-SEC−D4, interpolated to M_i from the ThFFF experiments as a fractogram for three different topologies. (b) Normalized differential weight distributions of the ThFFF data given in (a), superimposed by the normalized differential weight distributions generated directly from the HT-SEC−D4 data.

temperature (calculated with the exact temperature profile as that reported in ref 35) of t_R by batch DLS experiments (DLS data are given in the SI). The molar masses, measured by MALS coupled to the ThFFF, were calculated with a $dndc^{-1}$ = 0.075 ± 0.002 mL g^{-1} for cwPE in CHX, measured in batch (see Figure S3, SI). The results obtained from the ThFFF separation, given in Figure 2 and summarized in Table 1, show for all polymer topologies a lower thermal diffusion compared to that of other polymers of a similar molar mass such as polystyrene (PS) in CHX,[43] but a retention behavior very similar to that of commercial PEs as obtained by high-temperature ThFFF investigations.[48]

At a first glance, no obvious relation between M_w and S_T or D_T could be found. However, a strong correlation of molecular parameters like the molar apparent density ρ_{app} and LCB_w (from HT-SEC−D4) to S_T has been found (see Figures 3 and S7, SI). Furthermore, the dependence of D_T on M_{Seg} given in Figure 3b indicates the independence of the molar mass for large linear polymers, which is in agreement with Giddings et al.[42]

The same report also shows the lack of dependence of D_T on the branching,[42] which was also noted for a linear block and mikto-arm star copolymers pair of the same composition.[44,46] Both findings are in contradiction to our results. The dependence on branching, however, has instead been observed in other studies, for example, for linear and star PSs[43] and for dendritic polyesters.[45] It has been posited that this discrepancy in behavior may be driven by the thermodynamic quality of the solvent, similar to the nonideal scaling behavior in thermal diffusion observed for copolymers in selective solvents.[58]

We observe a significant influence of the polymer topology on the thermal diffusion behavior in our polymer−solvent system. The calculated thermal diffusion coefficients given in Table 1 directly correlate to the contraction factor g and the number of branches per molecule, calculated by eq 2 from HT-SEC−D4 data, respectively. The data shown in Figure 3c indicate the trend that D_T may become independent of the molar mass for larger linear segments. Furthermore, it also shows a clear dependence of the decreasing M_{Seg} with a trend toward decreasing D_T values, which would describe a thermophilic behavior for short linear segments. Both findings are in agreement with those of Köhler and Stadelmaier, who found a thermophilic behavior for *n*-alkanes and other mono-/oligomers in various solvents and a thermophobic behavior of their analogue polymers[32] by thermal-diffusion-forced Rayleigh scattering.[32,33,41,59] However, the trend of D_T for hydrocarbons to higher molar masses was not investigated due to the lack of polymers being readily soluble in the same solvent. It can be concluded that the thermal diffusion may be dependent on the effective size of a polymer segment where $M_{Seg} \ll M_w$.

Branching Analysis by ThFFF. The clearly found dependence of S_T and D_T on the polymer topology allows the development of a branching characterization approach by ThFFF. Similar to g and g', Runyon proposed the introduction of a Soret contraction factor g'',[46] defined as follows

DOI: 10.1021/acs.macromol.9b01410
Macromolecules 2019, 52, 8662−8671

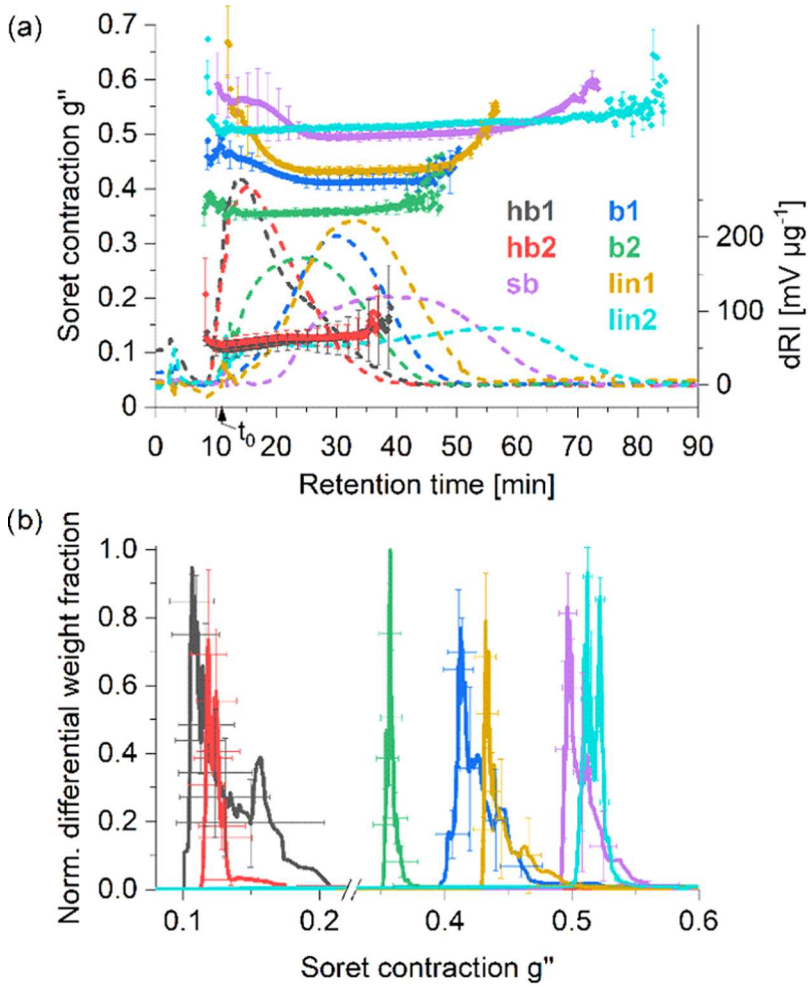

Figure 8. Superimposed generated data of g'' (a) as fractograms and (b) the derived normalized differential weight distributions for the fully relaxed system at a high field strength (ΔT = 100.9 K, τ = 10 min).

$$g'' = \left(\frac{S_{T,BRA}}{S_{T,LIN}}\right)_M \tag{8}$$

where $S_{T,BRA}$ is the Soret coefficient of the branched analyte and $S_{T,LIN}$ of the linear analogue with the same molar mass. For polymers with branching units, such as star-like structures or polymers consisting of an AB_2-type monomer,[60] a direct comparison with a linear analogue is applicable.[45] However, for cwPE, thermal diffusion properties of an entirely linear analogue soluble under the same conditions are not directly accessible. Furthermore, the previously used approach to calculate $S_{T,LIN}$ from a calibration of the molar mass versus retention time[61] of an almost linear sample in this case was not applicable due to the very narrow dispersity of the cwPE samples as a result of the synthesis conditions and the reaction mechanism.[22,53,62] Thus, a linear model has to be developed. Based on the observed direct dependence of S_T on the segmental molar mass (Figure S7d), a temperature-dependent model using the reciprocal of λ has been developed, as exemplarily shown in Figure 4 for the fully relaxed system, measured at a high field strength. The model parameters for the partially relaxed system without stop-flow (τ = 0 min) and for the fully relaxed system (τ = 10 min), measured at two different field strengths, are given in the SI. Due to deviation of the dRI data, the average retention time of the dRI and MALS peak apexes were used.

The fit parameters of λ^{-1} vs M_{Seg} were assumed to correspond to a linear dependence. Thus, a general model for the Soret coefficient of the linear analogue by extrapolation of M_{Seg} to M_w was developed, leading to a relation between $S_{T,LIN}$ and M_w, as given in eq 12.

$$S_{T,LIN} = \frac{(a_1 \cdot \Delta T + a_2) \cdot \ln M_w - (a_3 \cdot \Delta T + a_4)}{\Delta T} \tag{9}$$

The coefficients of eq 9 are given in Table S2 in the SI. According to the model described in eq 9, S_T reaches a plateau at a very high M_w and shows negative values in the oligomeric region of M_w, describing a thermophilic behavior. The tendency of S_T in the log (S_T) to log (M_w) plot to level-off for high molar masses has been described for PS in various solvents[63] over a wide range of M_w values,[64] but is less pronounced as we observed here. Consequently, it is considered to be dependent on the polymer−solvent system.

The obtained Soret contraction factors $g''(t_{R,dRI\ apex})$ summarized in Table 2 contain branching information analogous to the radius contraction factor determined by HT-SEC−D4. To calculate LCB from the ThFFF data as directly comparable to those from SEC-MALS, g'' needs to be transformed into g. As can be seen in Figure 5, g and g'' show a

DOI: 10.1021/acs.macromol.9b01410
Macromolecules 2019, 52, 8662−8671

correlation similar to the relation $g' = g^{\varepsilon}$. The concept with a single exponent could be also applied in $g'' = g^{\xi}$ by the introduction of a thermal drainage parameter ξ. The ξ from $g''(t_{R,dRI\ apex}) = (g_{HT\text{-}SEC-D4})^{\xi}$ yields values between 0.8 and 1.6, which is comparable to the typical range of ε between 0.5 and 1.5.[14] However, similar to ε, ξ seems to also depend on branching, which then would need to be described by a second independent variable related to branching, such as t_R or R. This may lead to a lower precision of the predicted g values due to the additional uncertainty contribution from the fit to the second variable. Therefore, a relation $g(g'')$ with only one variable has been developed, as described in eq 10. The transformation of g'' to g needs to fulfill the boundary condition of $g(g''= 1) = 1$. Thus, the fit of $g(g'')$ had to be realized by a more complex double Boltzmann fit.

$$g(g'') = K_1 + (K_2 - K_1)\left[\frac{K_3}{1 + 10^{(K_4 - g'')K_5}} + \frac{1 - K_3}{1 + 10^{(K_6 - g'')K_7}}\right] \quad (10)$$

The calculation of the values of the coefficient $K_x(\Delta T)$ is given in Tables S3−1 and S3−2 in the SI. The results found using eqs 8−10, summarized in Table 2 as average results from $t_{R,dRI\ apex}$, show a very good agreement between the calculated LCB[$g(g'')$] and LCB_w from HT-SEC−D4 as given in Table 1.

More information is expected to be gained by analyzing the entire ThFFF fractograms of the cwPE system. However, a determination of $S_{T,i}$ and g''_i for each slice at a certain retention time t_R or R was not directly accessible due to the unavailability of a sufficiently sensitive instrument to measure D online. This is also expected to be challenging due to the low dn/dc^{-1} of the polymers to the solvent and the low analyte concentration. Furthermore, the reverse application of the ThFFF approach given in eq 7 does not include the broadening of the analyte peak and can only display a discrete S_T value, for example, at the peak apex. Therefore, an indirect way has been developed to calculate $g''_i(R)$ eq 11 by application of the concept for $S_{T,LIN}$ eq 9 with a calculated molar mass of a segment for each slice, $M_{Seg,i}(R)$.

$$g''_i(R) = \left[\frac{S_{T,BRA}(M_{Seg,i})}{S_{T,LIN}(M_i)}\right]_{M_i} \quad (11)$$

For well-retained analytes, the calculation of $LCB_i(R)$ (calculated from $g''_i(R)$) with $M_{Seg} = M_i(R)\ (2B_{apex} + 1)^{-1}$ according to eq 4 was found to be in good agreement with $LCB_i(M_i)$ determined by HT-SEC−D4, which were numerically interpolated to M_i measured in the ThFFF fractionations. Here, the number average of B found by SEC was accounted to be the main fraction of the analyte at the peak apex (B_{apex}). However, $LCB_i(R)$ of poorly retained analytes could not be sufficiently described with the original definition of M_{Seg}. By implementing an empirically found correction in the definition of $M_{Seg,i}(R)$ eq 12, a satisfactory calculation of $LCB_i(R)$ in the entire retention range was achieved, resembling the values of $LCB_i(M_i)$ from HT-SEC−D4 interpolated to M_i of the ThFFF fractograms. The detailed development of eq 12 is described in the SI.

$$M_{Seg,i}(R) = \frac{R_{apex} \cdot M_{apex} + (1 - R_{apex})M_i(R)}{\left(2 - \frac{R^2}{e^R}\right)B_{apex} + 1} \quad (12)$$

To enable the calculation of $LCB_i(R)$ also for unknown analytes, a substitution for B_{apex} is required. Analogous to the previously shown dependence of D_T on B in Figure 3, a fit of B directly to the average of R_{MALS} and R_{dRI} was performed.

The data of B_{apex} shown in Figure 6 were found to resemble $LCB_{i,\ ThFFF}(R)$ on $LCB_{i,\ HT\text{-}SEC-D4}(M_{i,\ ThFFF})$ in good accuracy after fitting by a five-parameter logistic function (see eq 13).

$$B_{apex}(R_{apex}) = K_1 + \frac{K_2 - K_1}{\left[1 + \left(\frac{K_3}{R}\right)^{K_4}\right]^{K_5}} \quad (13)$$

The values of the coefficient $K_x(\Delta T)$ of eq 13 for the partially relaxed and fully relaxed systems are given in Tables S4−1 and S4−2 in the SI.

The application of the concept for the branching analysis, given by eqs 9−13, on the recorded data in the ThFFF separations shown in Figure 2 with $M_i(t_R)$, ΔT, and the cold wall temperature T_c is able to generate "online" data for LCB in correlation to t_R and is in reasonably good agreement to the LCB data from HT-SEC−D4, interpolated to $M_{i,\ ThFFF}$, as indicated in Figure 7a. The comparison of the normalized differential weight distribution indicates a good performance of the concept to analyze LCB for cwPEs of a more linear topology and a reasonable performance for highly branched topologies of analytes with a narrow and slightly broader dispersity. It also takes into account the effect of band broadening in an indirect way. Due to the non-Gaussian shape of the fractogram peak especially for poorly retained analytes, a band-broadening correction as described earlier[65,66] was considered not to be applicable for all analytes of this system; therefore, a mathematical consideration of band broadening is beyond the scope of this work. Furthermore, the molar mass dispersities $Đ$ reported in Table 1 were found to be marginally narrower compared to those obtained by SEC since SEC is discussed in the literature to slightly overestimate narrowly dispersed polymers,[66−68] and this also indicates that the band broadening may not have negatively affected the analysis. An improvement of the concept by a deeper understanding of the relation found between g and g'' is believed to deliver results with a higher accuracy.

Based on the output for $LCB_{i,\ ThFFF}(t_R)$ being in good agreement with the interpolated data of the HT-SEC−D4 analysis as illustrated in Figure, the reliability of the predictive generation of online data in correlation to t_R was considered to be accurate enough for the fractogram and distribution analysis of g''. As illustrated in Figure 8, the Soret contraction factor g'' shown together with the fractograms could be displayed with respect to the dispersities of the analytes. The generation of online data by application of the developed solution given in eqs 11−13 was found to be certainly accurate for an online branching analysis of the cwPE samples as a model in this investigation. It is also able to generate sufficiently correct data for unknown samples, which have not been part of the fitting process in the model development (see Figure S16 and Table S6). However, for broadly distributed systems in terms of M_w and branching, only an online determination by a separate detection is believed to generate reliable data for a true online branching analysis. For that, the temperature dependence of D needs to be determined either by heating the detector flow cell to the expected mean layer temperature or by the calculation of D measured at a fixed temperature. If the analyte concentration is too low for a reliable measurement of D by online-DLS, an

DOI: 10.1021/acs.macromol.9b01410
Macromolecules 2019, 52, 8662−8671

indirect determination by online viscometry could be an alternative. However, a systematic error needs to be taken into account, because R_h and the viscometric radius R_η, both sphere-equivalent radii, may differ for various polymers and topologies.[10,69]

CONCLUSIONS

Based on a model system of seven PE samples with varied molecular architectures (topologies) being produced by chain walking catalysis, an alternative approach for a branching analysis by ThFFF coupled to MALS and dRI detection has been developed in the context of the recently proposed concept of the Soret contraction. For this, a model to predict S_T for linear analogues of the same M_w has been introduced. The evaluation of this approach, either based on the mean retention time or with the help of an indirect method for the analysis of fractograms of narrowly dispersed samples, was found to be in good agreement with the reference data determined by HT-SEC−D4, representing the established approach for the branching analysis of polyolefins in general. It is believed that the new approach generally holds for commercial PEs as well as for similar polymers soluble only at elevated temperatures. However, this may need re-evaluations of the relationship of S_T vs M_{Seg} and g vs g'', and additionally, the analysis of broadly dispersed samples requires an online detection of D.

ASSOCIATED CONTENT

Supporting Information

The Supporting Information is available free of charge on the ACS Publications website at DOI: 10.1021/acs.macromol.9b01410.

Experimental details; HT-SEC−D4 results; temperature-dependent DLS experiments in batch; ThFFF data from different ΔT and τ; numerical solution of eq 7 for λ; development of eq 12; and cumulative and differential weight distributions of LCB and g'' (PDF)

AUTHOR INFORMATION

Corresponding Author

*E-mail: lederer@ipfdd.de.

ORCID

S. Kim Ratanathanawongs Williams: 0000-0003-3894-478X

Albena Lederer: 0000-0002-1760-6426

Author Contributions

The manuscript was written through contributions of all authors. All authors have given approval to the final version of the manuscript.

Notes

The authors declare no competing financial interest.

ACKNOWLEDGMENTS

This work was supported by the Deutsche Forschungsgemeinschaft (DFG, German Research Foundation) [grant number DFG LE 1424/7], the Czech Science Foundation [15-15887J and 18-22059S], the National Science Foundation (NSF) [CHE-150882, CHE-1808805], and Fulbright (SKRW). We thank Petra Treppe and Christina Harnisch for their technical assistance.

REFERENCES

(1) Thayer, A. M. Metallocene Catalysts Initiate New Era In Polymer Synthesis. *Chem. Eng. News* **1995**, *73*, 15−20.

(2) Ittel, S. D.; Johnson, L. K.; Brookhart, M. Late-Metal Catalysts for Ethylene Homo- and Copolymerization. *Chem. Rev.* **2000**, *100*, 1169−1204.

(3) Knuuttila, H.; Lehtinen, A.; Nummila-Pakarinen, A. Advanced Polyethylene Technologies---Controlled Material Properties. In *Long Term Properties of Polyolefins*; Albertsson, A.-C., Ed.; Springer: Berlin, Heidelberg, 2004; pp 13−28.

(4) Macko, T.; Brüll, R.; Zhu, Y.; Wang, Y. A Review on the Development of Liquid Chromatography Systems for Polyolefins. *J. Sep. Sci.* **2010**, *33*, 3446−3454.

(5) Wild, L.; Glöckner, G. In*Temperature Rising Elution Fractionation BT - Separation Techniques Thermodynamics Liquid Crystal Polymers*; Springer: Berlin, Heidelberg, 1991; pp 1−47.

(6) Monrabal, B. Crystallization Analysis Fractionation: A New Technique for the Analysis of Branching Distribution in Polyolefins. *J. Appl. Polym. Sci.* **1994**, *52*, 491−499.

(7) Wild, L.; Guliana, R. Gel Permeation Chromatography of Polyethylene: Effect of Long-Chain Branching. *J. Polym. Sci., Part A-2.* **1967**, *5*, 1087−1101.

(8) Crouzet, P.; Fine, F.; Mangin, P. Comparaison Des Méthodes de Fractionnement Par Chromatographie de Perméation et Par Gradient d'elution Pour La Détermination Des Répartitions Moléculaires Des Polypropylénes. *J. Appl. Polym. Sci.* **1969**, *13*, 205−213.

(9) Boborodea, A.; Collignon, F.; Brookes, A. Characterization of Polyethylene in Dibutoxymethane by High-Temperature Gel Permeation Chromatography with Triple Detection. *Int. J. Polym. Anal. Charact.* **2015**, *20*, 316−322.

(10) Plüschke, L.; Mundil, R.; Sokolohorskyj, A.; Merna, J.; Sommer, J.-U.; Lederer, A. High Temperature Quadruple-Detector Size Exclusion Chromatography for Topological Characterization of Polyethylene. *Anal. Chem.* **2018**, *90*, 6178−6186.

(11) Zimm, B. H.; Stockmayer, W. H. The Dimensions of Chain Molecules Containing Branches and Rings. *J. Chem. Phys.* **1949**, *17*, 1301−1314.

(12) Stockmayer, W. H.; Fixman, M. DILUTE SOLUTIONS OF BRANCHED POLYMERS. *Ann. N. Y. Acad. Sci.* **1953**, *57*, 334−352.

(13) Zimm, B. H.; Kilb, R. W. Dynamics of Branched Polymer Molecules in Dilute Solution. *J. Polym. Sci.* **1959**, *37*, 19−42.

(14) Lederer, A.; Burchard, W.; Khalyavina, A.; Lindner, P.; Schweins, R. Is the Universal Law Valid for Branched Polymers? *Angew. Chem., Int. Ed.* 2013, *52* (17), 4659−4663. DOI: 10.1002/anie.201209228

(15) Lederer, A.; Burchard, W.; Hartmann, T.; Haataja, J. S.; Houbenov, N.; Janke, A.; Friedel, P.; Schweins, R.; Lindner, P. Dendronized Hyperbranched Macromolecules: Soft Matter with a Novel Type of Segmental Distribution. *Angew. Chem., Int. Ed.* 2015, *54* (43), 12578−12583. DOI: 10.1002/anie.201504059

(16) Gabriel, C.; Münstedt, H. Influence of Long-Chain Branches in Polyethylenes on Linear Viscoelastic Flow Properties in Shear. *Rheol. Acta* **2002**, *41*, 232−244.

(17) Krause, B.; Voigt, D.; Häußler, L.; Auhl, D.; Münstedt, H. Characterization of Electron Beam Irradiated Polypropylene: Influence of Irradiation Temperature on Molecular and Rheological Properties. *J. Appl. Polym. Sci.* **2006**, *100*, 2770−2780.

(18) Guan, Z. Chain Walking: A New Strategy to Control Polymer Topology. *Science* **1999**, *283*, 2059−2062.

(19) Johnson, L. K.; Killian, C. M.; Brookhart, M. New Pd(II)- and Ni(II)-Based Catalysts for Polymerization of Ethylene and.Alpha.-Olefins. *J. Am. Chem. Soc.* **1995**, *117*, 6414−6415.

(20) Patil, R.; Colby, R. H.; Read, D. J.; Chen, G.; Guan, Z. Rheology of Polyethylenes with Novel Branching Topology Synthesized by a Chain-Walking Catalyst. *Macromolecules* **2005**, *38*, 10571−10579.

(21) Cotts, P. M.; Guan, Z.; McCord, E.; McLain, S. Novel Branching Topology in Polyethylenes As Revealed by Light Scattering and 13C NMR. *Macromolecules* **2000**, *33*, 6945−6952.

DOI: 10.1021/acs.macromol.9b01410
Macromolecules 2019, 52, 8662−8671

(22) Dockhorn, R.; Plüschke, L.; Geisler, M.; Zessin, J.; Lindner, P.; Mundil, R.; Merna, J.; Sommer, J.-U.; Lederer, A. Polyolefins Formed by Chain Walking Catalysis—A Matter of Branching Density Only? *J. Am. Chem. Soc.* **2019**, *141*, 15586−15596.
(23) Schallausky, F.; Erber, M.; Komber, H.; Lederer, A. An Easy Strategy for the Synthesis of Well-Defined Aliphatic-Aromatic Hyperbranched Polyesters. *Macromol. Chem. Phys.* **2008**, *209*, 2331−2338.
(24) Khalyavina, A.; Häußler, L.; Lederer, A. Effect of the Degree of Branching on the Glass Transition Temperature of Polyesters. *Polymer* **2012**, *53*, 1049−1053.
(25) Striegel, A. M.; Yau, W. W.; Kirkland, J. J.; Bly, D. D. Retention. In *Modern Size-Exclusion Liquid Chromatography*; Wiley Online Books: 2009; p 496.
(26) Podzimek, S.; Vlcek, T.; Johann, C. Characterization of Branched Polymers by Size Exclusion Chromatography Coupled with Multiangle Light Scattering Detector. I. Size Exclusion Chromatography Elution Behavior of Branched Polymers. *J. Appl. Polym. Sci.* **2001**, *81*, 1588−1594.
(27) Erber, M.; Boye, S.; Hartmann, T.; Voit, B. I.; Lederer, A. A Convenient Room Temperature Polycondensation toward Hyperbranched AB2-Type All-Aromatic Polyesters with Phenol Terminal Groups. *J. Polym. Sci., Part A: Polym. Chem.* **2009**, *47*, 5158−5168.
(28) Schimpf, M. E.; Caldwell, K.; Giddings, J. C. *Field-Flow Fractionation Handbook*; John Wiley & Sons, Inc., 2000; pp 3−48.
(29) Ludwig, C. Diffusion Zwischen Ungleich Erwärmten Orten Gleich Zusammengesetzter Lösungen *Sitzungber Bayer Akad Wiss Wien Math-Naturwiss Kl* 1856, *20*, 539.
(30) Soret, C. Sur l'état d'équilibre Que Prend, Au Point de Vue de Sa Concentration, Une Dissolution Saline Primitivement Homogène, Dont Deux Parties Sont Portées à Des Températures Différentes. *J. Phys. Theor. Appl.* **1880**, *9*, 331−332.
(31) Eslamian, M.; Ziad, S. M. A Critical Review of Thermodiffusion Models: Role and Significance of the Heat of Transport and the Activation Energy of Viscous Flow. *J. Non-Equilib. Thermodyn.* **2009**, *34*, 97.
(32) Stadelmaier, D.; Köhler, W. Thermal Diffusion of Dilute Polymer Solutions: The Role of Chain Flexibility and the Effective Segment Size. *Macromolecules* **2009**, *42*, 9147−9152.
(33) Morozov, K. I.; Köhler, W. Thermophoresis of Polymers: Nondraining vs Draining Coil. *Langmuir* **2014**, *30*, 6571−6576.
(34) Van Asten, A. C.; Boelens, H. F. M.; Kok, W. T.; Poppe, H.; Williams, P. S.; Giddings, J. C. Temperature Dependence of Solvent Viscosity, Solvent Thermal Conductivity, and Soret Coefficient in Thermal Field-Flow Fractionation. *Sep. Sci. Technol.* **1994**, *29*, 513−533.
(35) Belgaied, J. E.; Hoyos, M.; Martin, M. Velocity Profiles in Thermal Field-Flow Fractionation. *J. Chromatogr. A* **1994**, *678*, 85−96.
(36) Williams, S. K. R.; Lee, D. Field-Flow Fractionation of Proteins, Polysaccharides, Synthetic Polymers, and Supramolecular Assemblies. *J. Sep. Sci.* **2006**, *29*, 1720−1732.
(37) Williams, S. K. R.; Runyon, J. R.; Ashames, A. A. Field-Flow Fractionation: Addressing the Nano Challenge. *Anal. Chem.* **2011**, *83*, 634−642.
(38) Qureshi, R. N.; Kok, W. T. Application of Flow Field-Flow Fractionation for the Characterization of Macromolecules of Biological Interest: A Review. *Anal. Bioanal. Chem.* **2011**, *399*, 1401−1411.
(39) Gunderson, J. J.; Giddings, J. C. Field-Flow Fractionation. In *Comprehensive Polymer Science*; Allen, G.; Bevington, J., Eds.; Pergamon Press: Oxford, 1989; p 279.
(40) Schimpf, M. E. Characterization of Polymers by Thermal Field-Flow Fractionation. *J. Chromatogr. A* **1990**, *517*, 405−421.
(41) Rauch, J.; Köhler, W. On the Molar Mass Dependence of the Thermal Diffusion Coefficient of Polymer Solutions. *Macromolecules* **2005**, *38*, 3571−3573.
(42) Schimpf, M. E.; Giddings, J. C. Characterization of Thermal Diffusion in Polymer Solutions by Thermal Field-Flow Fractionation: Effects of Molecular Weight and Branching. *Macromolecules* **1987**, *20*, 1561−1563.
(43) Greyling, G.; Lederer, A.; Pasch, H. Thermal Field-Flow Fractionation for the Investigation of the Thermoresponsive Nature of Star and Linear Polystyrene. *Macromol. Chem. Phys.* **2018**, *219*, No. 1800417.
(44) Runyon, J. R.; Williams, S. K. R. Composition and Molecular Weight Analysis of Styrene-Acrylic Copolymers Using Thermal Field-Flow Fractionation. *J. Chromatogr. A* **2011**, *1218*, 6774−6779.
(45) Smith, W. C.; Geisler, M.; Lederer, A.; Williams, S. K. R. Thermal Field-Flow Fractionation for Characterization of Architecture in Hyperbranched Aromatic-Aliphatic Polyesters with Controlled Branching. *Anal. Chem.* **2019**, *91*, 12344−12351.
(46) Runyon, J. R. *Thermal Field-Flow Fractionation of Polymers with High Molecular Weight and Complex Architectures*; Colorado School of Mines: Golden, CO, 2009.
(47) Brimhall, S. L.; Myers, M. N.; Caldwell, K. D.; Giddings, J. C. High Temperature Thermal Field-Flow Fractionation for the Characterization of Polyethylene. *Sep. Sci. Technol.* **1981**, *16*, 671−689.
(48) Pasti, L.; Roccasalvo, S.; Dondi, F.; Reschiglian, P. High Temperature Thermal Field-Flow Fractionation of Polyethylene and Polystyrene. *J. Polym. Sci., Part B: Polym. Phys.* **1995**, *33*, 1225−1234.
(49) Horská, J.; Stejskal, J.; Kratochvíl, P. Refractive Index Increments of Polyethylene. *J. Appl. Polym. Sci.* **1979**, *24*, 1845−1855.
(50) MacRury, T. B.; McConnell, M. L. Measurement of the Absolute Molecular Weight and Molecular Weight Distribution of Polyolefins Using Low-Angle Laser Light Scattering. *J. Appl. Polym. Sci.* **1979**, *24*, 651−662.
(51) Sun, T.; Brant, P.; Chance, R. R.; Graessley, W. W. Effect of Short Chain Branching on the Coil Dimensions of Polyolefins in Dilute Solution. *Macromolecules* **2001**, *34*, 6812−6820.
(52) Wood-Adams, P. M.; Dealy, J. M.; deGroot, A. W.; Redwine, O. D. Effect of Molecular Structure on the Linear Viscoelastic Behavior of Polyethylene. *Macromolecules* **2000**, *33*, 7489−7499.
(53) Mundil, R.; Hermanová, S.; Peschel, M.; Lederer, A.; Merna, J. On the Topology of Highly Branched Polyethylenes Prepared by Amine−imine Nickel and Palladium Complexes: The Effect of Ortho-Aryl Substituents. *Polym. Int.* **2018**, *67*, 946−956.
(54) Hansen, C. M.; Durkee, J.; Kontogeorgis, G.; Panayiotou, C.; Willliams, L. L.; Poulsen, T. S.; Priebe, H.; Redelius, P. *Hansen Solubility Parameters: A User's Handbook, Second Edition*, 2nd ed.; CRC Press: 2007; pp 75−110 and 345−507
(55) Stepto, R. F. T. Dispersity in Polymer Science (IUPAC Recommendations 2009). *Pure Appl. Chem.* **2009**, *81*, 351.
(56) Stepto, R. F. T. Erratum. *Pure Appl. Chem.* **2009**, *81*, 351−353.
(57) Lansing, W. D.; Kraemer, E. O. Molecular Weight Analysis of Mixtures by Sedimentation Equilibrium in the Svedberg Ultracentrifuge. *J. Am. Chem. Soc.* **1935**, *57*, 1369−1377.
(58) Schimpf, M. E.; Giddings, J. C. Characterization of Thermal Diffusion of Copolymers in Solution by Thermal Field-Flow Fractionation. *J. Polym. Sci., Part B: Polym. Phys.* **1990**, *28*, 2673−2680.
(59) Köhler, W. Thermodiffusion in Polymer Solutions as Observed by Forced Rayleigh Scattering. *J. Chem. Phys.* **1993**, *98*, 660−668.
(60) Khalyavina, A.; Schallausky, F.; Komber, H.; Al Samman, M.; Radke, W.; Lederer, A. Aromatic−Aliphatic Polyesters with Tailored Degree of Branching Based on AB/AB2 and ABB*/AB2 Monomers. *Macromolecules* **2010**, *43*, 3268−3276.
(61) Nguyen, M.; Beckett, R. Calibration Methods for Field-Flow Fractionation Using Broad Standards. I. Thermal Field-Flow Fractionation. *Sep. Sci. Technol.* **1996**, *31*, 291−317.
(62) Gottfried, A. C.; Brookhart, M. Living Polymerization of Ethylene Using Pd(II) α-Diimine Catalysts. *Macromolecules* **2001**, *34*, 1140−1142.
(63) Giddings, J. C.; Caldwell, K. D.; Myers, M. N. Thermal Diffusion of Polystyrene in Eight Solvents by an Improved Thermal Field-Flow Fractionation Methodology. *Macromolecules* **1976**, *9*, 106−112.

DOI: 10.1021/acs.macromol.9b01410
Macromolecules 2019, 52, 8662−8671

(64) Gao, Y. S.; Caldwell, K. D.; Myers, M. N.; Giddings, J. C. Extension of Thermal Field-Flow Fractionation to Ultra-High (20.Times. 106) Molecular Weight Polystyrenes. *Macromolecules* **1985**, *18*, 1272−1277.
(65) Schimpf, M. E.; Williams, P. S.; Giddings, J. C. Accurate Molecular Weight Distribution of Polymers Using Thermal Field-Flow Fractionation with Deconvolution to Remove System Dispersion. *J. Appl. Polym. Sci.* **1989**, *37*, 2059−2076.
(66) Schimpf, M. E.; Myers, M. N.; Giddings, J. C. Measurement of Polydispersity of Ultra-Narrow Polymer Fractions by Thermal Field-Flow Fractionation. *J. Appl. Polym. Sci.* **1987**, *33*, 117−135.
(67) Lee, W.; Lee, H.; Cha, J.; Chang, T.; Hanley, K. J.; Lodge, T. P. Molecular Weight Distribution of Polystyrene Made by Anionic Polymerization. *Macromolecules* **2000**, *33*, 5111−5115.
(68) Lee, H. C.; Chang, T. Polymer Molecular Weight Characterization by Temperature Gradient High Performance Liquid Chromatography. *Polymer* **1996**, *37*, 5747−5749.
(69) Brewer, A. K.; Striegel, A. M. Particle Size Characterization by Quadruple-Detector Hydrodynamic Chromatography. *Anal. Bioanal. Chem.* **2009**, *393*, 295.

DOI: 10.1021/acs.macromol.9b01410
Macromolecules 2019, 52, 8662−8671